IEEE Access
Multidisciplinary | Rapid Review | Open Access Journal

Received 8 July 2023, accepted 15 August 2023, date of publication 21 August 2023, date of current version 5 September 2023.

Digital Object Identifier 10.1109/ACCESS.2023.3307137

RESEARCH ARTICLE

Elliptical Circumnavigation for Multiple Quadrotors With Regulatable Intervehicle Distance: Experimental Validation

HAO CHEN[1], XINGLING SHAO[2], (Member, IEEE), AND RUIQING JIA[1]
[1]School of Mechanical Electronic and Information Engineering, China University of Mining and Technology (Beijing), Beijing 100083, China
[2]School of Instrument and Electronics, North University of China, Taiyuan 030051, China

Corresponding author: Hao Chen (bqt1800402011@student.cumtb.edu.cn)

This work was supported in part by the National Natural Science Foundation of China under Grant 61603353, and in part by the Fund for the Shanxi 1331 Project Key Subjects Construction under Grant 1331KSC.

ABSTRACT This article presents an elliptical circumnavigation control strategy for multiple quadrotors subject to uncertainties. At translational level, a novel horizontal elliptical guidance law capable of regulating the relative distance between different quadrotors and a vertical control law are synchronized to educe the translation controller. At rotational level, an USDE characterized by laconic constructure and simple parameter tuning, is introduced to estimate the unknown lumped uncertainties online. The primary advantage of this paper is that the elliptical circumnavigation with regulatable distance between circling quadrotors is achieved. Meanwhile, all the error signals in the closed-loop system are analyzed to be bounded. Finally, practical experiments verify the efficacy of suggested strategy.

INDEX TERMS Elliptical circumnavigation, moving target, unknown system dynamics estimator, circular formation, adjustable intervehicle distance, quadrotors.

I. INTRODUCTION

21st century is the century of flight, more and more countries are devoting to the development of control technology for unmanned aerial vehicles (UAVs) [1], [2], [3], [4], [5]. As the brand representative, quadrotor UAVs have been deemed as a powerful tool to accomplish tough missions as mapping, location, detection, transporting, agricultural irrigation and so on. Differing from classic path following [6], trajectory tracking [7] or attitude tracking [8], target encircling control for quadrotors has become a promising topic [9], [10], which drives quadrotors to circularly fly around a certain target along with a predesigned relative distance. Thus, how to conduct effective and robust satisfactory target encircling controller for quadrotors is a meaningful but challenging issue, especially in assuring accuracy target tracking, circling motion as well as disturbance rejection.

Aiming at achieving a robust and accurate encircling, fruitful innovative target encircling control recipes have been conducted [9], [10], [11], [12]. In [13], a cyclic control policy is suggested for monitoring the single static target. Based on quadrotor velocity and relative distance between quadrotors and target, a circumnavigation control methodology with unknown target is advanced for quadrotors [14]. By fusion of finite-time control law, non-holonomic robots are allowed to circumnavigate the targets in finite time without considering uncertainties [15]. By modeling the target movement with a finite-state Markov chain, a discrete-time Lyapunov guidance vector field (LGVF) is created for guiding and controlling quadrotors to encircle over the moving target [16]. Note that most aforementioned achievements [13], [14], [15], [16] focus on target circumnavigation with a single agent, whose dexterity and investigation ability for target are limited compared to multiple agents. A fleet of quadrotors are able to achieve a more excellent target tracking encircling performance and provide more comprehensive objective information from various views. Although multi-agent inevitably renders considerable challenge for controller design, especially for the cooperativeness among different agents, tremendous efforts have been made to accomplish high-performance

The associate editor coordinating the review of this manuscript and approving it for publication was Haibin Sun.

cooperative target circumnavigation. In [17], a speed-based controller is conduced to regulate the intervehicle position, such that the target circumnavigation with certain phase intervals is achieved for a UAV team. To improve the disturbance rejection ability of quadrotor UAVs, an extended state observer (ESO) is synthetized into the cooperative target formation circling controller, such that a robust circumnavigation for targets is guaranteed [18]. Unfortunately, the forgoing encircling schemes are often falling short in terms of flexibility, observation efficiency and adaptiveness against intricate aerial sense due to their permanently constant surrounding radius. In order to resolve such drawback, an elliptical orbit control scheme for multiple objects is derived in [19], showing its outstanding flexible and approximative circumnavigation performance. Nevertheless, as previous multiple agents circling scenarios, mechanical crashes will be unavoidably induced because of the increasement of agents. Although some works of art have been proposed to resolve such problem by regulating the phase angle between agents [20], the relative distances are hard to reveal because of the complicated elliptical trace. Furthermore, one should note that the suggested target circumnavigation schemes pay little attention to uncertainties, indicating that the encircling mission may fail once the quadrotors encounter extraneous disturbances. Thus, it is of great academic and engineering value to deduce an elliptical circumnavigation controller with enhanced disturbance-rejection capability for quadrotor formulation.

With the aim of reinforcing the robustness of the quadrotors, disturbance observer-based is a currently prevailing and effective choose. So far, abundant of valid disturbance observers have been reported for quadrotors, containing ESO [18], [21], neural network (NN) observer [21], sliding mode observer [23], unknown system dynamics estimator (USDE) [24], [25], [26], etc. Among which, USDE is famous for its brief constructure, straightforward parameter tuning and low computation consumption, which renders its effective implementation on various platforms [24], [25], [26]. Originated in the philosophy of invariant manifold, USDE is firstly tackled to estimate the neutralize the unknown uncertainties of a robot system [24]. In [25], the USDE is incorporated into a sliding mode control scheme for a servo system suffering from both internal and extraneous disturbances, demonstrating a precise estimation ability. Moreover, the successful accomplishment on quadrotor attitude subsystem significantly reveals the excellent merits of USDE [26]. Hence, applying USDE on quadrotors is contributive and valued to overcome the drawbacks in elliptical encircling control of quadrotors.

Motivated by investigation above, herein an elliptical encircling control strategy incorporated with USDE is suggested for multiple quadrotors to achieve cooperative circumnavigation around a target along with a pregiven elliptical circle, whose superiorities can be concluded as below:

1) Differing from prevailing circumnavigation results [20] whose circling orbit radius is permanent, restricting the working environment, herein an elliptical encircling controller with an inconstant distance to target is derived for quadrotors, meeting more general working requirements. In advance, proposed controller can avert collision by regulating the distance between quadrotors rather than phase, which is more universal to real practice.

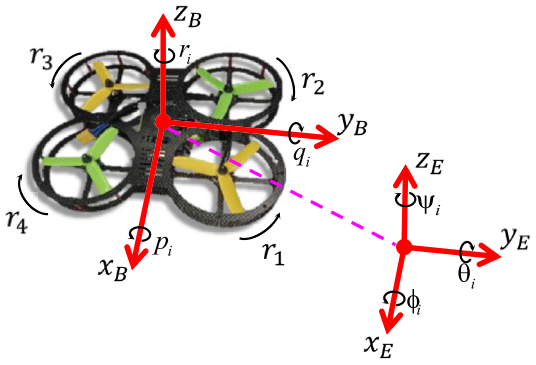

FIGURE 1. Illustration of i^{th} quadrotors in team.

2) A USDE is adopted to rebuild the unknown uncertainties degrading encircling performance. Following the philosophy of invariant manifold, USDE necessitates filtering operation on the measurable quadrotor dynamics with tuning merely one parameter, extremely saving burdensome computation compared to NN-based observers. Moreover, an asymptotic convergence is achieved once the filter constant is small enough, exhibiting a superior estimation ability.

Remainder of this article is arranged as below. Section II gives the preliminaries and problem formulation. Design of the elliptical encircling controller is stated in Section III. Corresponding stability analysis is analyzed in Section IV. Experiment results with corresponding analyses are given in Section V. Section VI concludes this paper.

II. PRELIMINARIES AND PROBLEM FORMULATION

A. NOTATION

Subsequent notations are used throughout this paper. $[\cdot]^T$ is a column vector. A diagonal matrix is expressed as diag$(\cdot)$. $|\cdot|$ refers to the absolute value of a real number. The 2-norm value of a vector/matrix is $\|\cdot\|$. $\mathbb{R}^{m\times n}$ is the set of real numbers, whose row and column are m and n, respectively. $s(\cdot)$ and $c(\cdot)$ are abbreviations of sin $(\cdot)$ and cos $(\cdot)$, respectively.

B. PROBLEM FORMULATION

For a quadrotor team containing N quadrotors, the constructure of the i^{th} quadrotors is plotted in Fig.1 ($i = 1, 2, 3\cdots, N$). Here, two coordinate frames, i.e., body frame $x_B - y_B - z_B$ and Earth frame $x_E - y_E - z_E$, are defined to represent the dynamics of quadrotors, where Euler angles are expressed by the vector $\mathbf{\Theta}_i = [\phi_i, \theta_i, \psi_i]^T \in \mathbb{R}^{3\times 1}$ under Earth-fixed frame with ϕ_i, θ_i and ψ_i denoting the roll, pitch and yaw angle, respectively. Angular velocity is expressed as $\mathbf{\Omega} = [p_i, q_i, r_i]^T \in \mathbb{R}^{3\times 1}$. The position under Earth-fixed

frame is described by $\boldsymbol{p}_i = \left[p_{ix}, p_{iy}, p_{iz}\right]^T \in \mathbb{R}^{3\times1}$, where position of target is $\boldsymbol{p}_t = \left[p_{tx}, p_{ty}\right]^T \in \mathbb{R}^{2\times1}$. Propellers endow the quadrotors to fulfill varied motions by producing thruster froce F_r $(r = 1, 2, 3, 4)$. The kinematics and kinetics of the i^{th} quadrotors in the team are formulated as

$$\begin{cases} \dot{\boldsymbol{p}}_i = \boldsymbol{v}_i \\ \dot{\boldsymbol{v}}_i = \left(\boldsymbol{K}_i u_{iF} - \boldsymbol{G}_i\right)/m_i \\ \dot{\boldsymbol{\Theta}}_i = \mathbf{W}_i \boldsymbol{\Omega}_i \\ \dot{\boldsymbol{\Omega}}_i = \mathbf{f}\left(\boldsymbol{\Omega}_i\right) + \mathbf{g}_{\boldsymbol{\Omega},i}\mathbf{M}_i + \mathbf{D}_i \end{cases} \tag{1}$$

where $\boldsymbol{v}_i = \left[v_{ix}, v_{iy}, v_{iz}\right]^T \in \mathbb{R}^{3\times1}$ is the linear velocity in Earth-fixed frame. $\boldsymbol{K}_i = [c\left(\psi_i\right)s\left(\theta_i\right)c\left(\phi_i\right) + s\left(\psi_i\right)s\left(\phi_i\right), s\left(\psi_i\right)s\left(\theta_i\right)c\left(\phi_i\right) - c\left(\psi_i\right)s\left(\phi_i\right), c\left(\theta_i\right)c\left(\phi_i\right)]^T \in \mathbb{R}^{3\times1}$, u_{iF} denotes the total propulsion force. The gravity effect is $\boldsymbol{G}_i = [0, 0, m_i g]^T \in \mathbb{R}^{3\times1}$,where m_i and g are the quadrotor weight and gravitational acceleration. $\mathbf{f}\left(\boldsymbol{\Omega}_i\right) = -\boldsymbol{I}^{-1}\boldsymbol{\Pi}_{\Omega_i}\boldsymbol{\Omega}_i \in \mathbb{R}^{3\times1}$ denotes the unknown nonlinear perturbation induced by parametric uncertainties with $\boldsymbol{I}_i = \mathrm{diag}(I_{ix}, I_{iy}, I_{iz}) \in \mathbb{R}^{3\times3}$ being the inertia matrix and $\boldsymbol{\Pi}_{\Omega_i} \in \mathbb{R}^{3\times3}$ being the unknown damping coefficient. $\mathbf{M}_i = [\mathrm{M}_{i1}, \mathrm{M}_{i2}, \mathrm{M}_{i3}]^T \in \mathbb{R}^{3\times1}$ stands for the control torque vector with $\boldsymbol{G}_{\Omega_i} = \mathrm{diag}(l_i/I_{ix}, l_i/I_{iy}, c_i/I_{iz}) \in \mathbb{R}^{3\times3}$, where l_i corresponds to the distance between propeller and the quadrotor barycenter and c_i represents the force-to-moment factor. $\mathbf{D}_i = [\mathrm{D}_{i1}, \mathrm{D}_{i2}, \mathrm{D}_{i3}]^T \in \mathbb{R}^{3\times1}$ is the extrinsic disturbance vector. And $\mathbf{W}_i$ is deemed as the transfer matrix from body frame to Earth frame, written in the form of

$$\mathbf{W}_i = \begin{pmatrix} 1 & \sin\phi_i \tan\theta_i & \cos\phi_i \tan\theta_i \\ 0 & \cos\phi_i & -\sin\phi_i \\ 0 & \sin\phi_i/\cos\theta_i & \cos\phi_i/\cos\theta_i \end{pmatrix}$$

Furthermore, let we have $\mathbf{x}_{i2} = \mathbf{W}_i\boldsymbol{\Omega}_i = [x_{i21}, x_{i22}, x_{i23}]^T$ and the quadrotor system could be updated from (1) to

$$\begin{cases} \dot{\boldsymbol{\Theta}}_i = \boldsymbol{x}_{i2} \\ \dot{\boldsymbol{x}}_{i2} = \underbrace{\dot{\mathbf{W}}_i\boldsymbol{\Omega}_i + \mathbf{W}_i\left(\mathbf{f}\left(\boldsymbol{\Omega}_i\right) + \mathbf{D}_i\right)}_{\boldsymbol{\Delta}_i} + \underbrace{\mathbf{W}_i\mathbf{g}_{\Omega,i}\mathbf{M}_i}_{\boldsymbol{\tau}_i} \end{cases} \tag{2}$$

$\boldsymbol{\Delta}_i = [\Delta_{i1}, \Delta_{i2}, \Delta_{i3}]^T \in \mathbb{R}^{3\times1}\Delta$ is the lumped disturbance and $\boldsymbol{\tau}_i = [\tau_{i1}, \tau_{i2}, \tau_{i3}]^T \in \mathbb{R}^{3\times1}$ represents the actual control input.

To achieve elliptical encircling motion of quadrotor team for a dynamic target, the general controller design could be roughly divided into two portions, i.e., horizontal and vertical portion. Fig.2 tells the relationship between the i^{th} quadrotors and target. $\boldsymbol{p}_{iH} = \left[p_{ix}, p_{iy}\right]^T \in \mathbb{R}^{2\times1}$ and $\rho_i = \left\|\boldsymbol{p}_t - \boldsymbol{p}_{iH}\right\|$ are the horizontal location of the i^{th} quadrotors and its planar distance to target. The unit vector from the i^{th} quadrotors to target is expressed in $\boldsymbol{\Phi}_i = \left(\boldsymbol{p}_t - \boldsymbol{p}_{iH}\right)/\rho_i = [\cos\beta_i, \sin\beta_i]^T$, where β_i is the bearing angle. The desired distance from the i^{th} quadrotors to target along with an elliptical trace is $\rho_{id}\left(t\right)$ with macro axis a and minor axis b, where ∂ is the contrarotating angle of identical ellipse and the relationship among ϑ_i, ∂ and β_i is formulated as

$$\vartheta_i - \partial = (2k+1)\,\pi, \quad k \in \mathbb{Z} \tag{3}$$

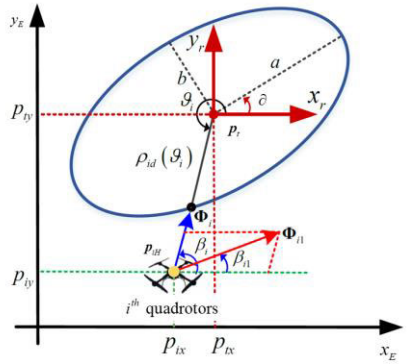

FIGURE 2. Position relationship between target and i^{th} quadrotors.

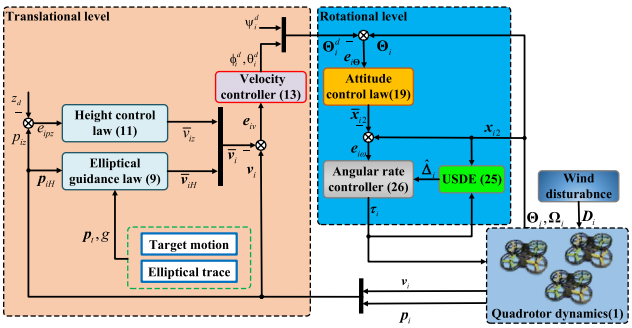

FIGURE 3. Architecture of presented control algorithm.

The normalized vector of the circumferential velocity of the i^{th} quadrotors is $\boldsymbol{\Phi}_{i1} = [\cos\beta_{i1}, \sin\beta_{i1}]^T$ with β_{i1} representing the angle between horizontal axis and tangential velocity direction.

Assumption 1: The velocity of target $\left\|\dot{\boldsymbol{p}}_t\right\|$ and the tangential velocity of the i^{th} quadrotors along with an elliptical trajectory v_i are both bounded, whose upper boundaries are positive constants, expressed by $\left\|\dot{\boldsymbol{p}}_t\right\| \le K_t$ and $|v_i| \le K_v$.

Control Objective: Our control goal aims at exploring an elliptical circumnavigation controller of quadrotor team for a moving target, allowing for with tunable intervehicle distance as well as improved robustness against uncertainties

a) The orbiting radius of quadrotors ρ_i can converge to a the ideal ρ_i with an adequately small error and intervehicle distances of different quadrotors are adjustable with sufficiently deviations, such that the mechanical collision is avoided.

b) The uncertainties can be rebuilt using USDE and corresponding, whose estimation error is assured to evolve within a sufficiently small set around the origin.

III. CONTROLLER DESIGN

In this section, the suggested elliptical circumnavigation controller will be explored for quadrotor team (2) and its overall control architecture is illustrated in Fig.2. Above all, a horizontal elliptical guidance law is deduced to achieve quadrotors enclosing to target as well as elliptical encircling with adjustable intervehicle distances. Subsequently, controller on rotational level is explored to track corresponding reference signal generated by an inverse decoupling transformation. The general control algorithm architecture is shown in Fig.3.

A. TRANSLATION LEVEL

1) HORIZONTAL GUIDANCE

As the prominent part, the elliptical orbiting motion of quadrotors, the ideal relative distance ρ_{id} as well as $\mathbf{\Phi}_{i1}$ are critical characteristics. Based on the standard elliptical trace, i.e., $p_{ix}^2/a^2 + p_{iy}^2/b^2 = 1$, then rotate the above ellipse ∂ degrees counterclockwise and one has

$$\frac{\left(p_{ix}\cos\partial + p_{iy}\sin\partial\right)^2}{a^2} + \frac{\left(p_{ix}\sin\partial - p_{iy}\cos\partial\right)^2}{b^2} = 1 \quad (4)$$

Note that ρ_{id} can be used to described any point on the ellipse as $[\rho_{id}(\vartheta_i)\cos\vartheta_i, \rho_{id}(\vartheta_i)\sin\vartheta_i]^T$, then ρ_{id} can be calculated based on (4) as:

$$\rho_{id}(\vartheta_i) = \frac{ab}{\sqrt{a^2\sin^2(\vartheta_i - \partial) + b^2\cos^2(\vartheta_i - \partial)}} \quad (5)$$

Subsequently, denote the g_{ix} and g_{iy} as the first-level partial derivative of $g\left(p_{ix}, p_{iy}\right) = \left(p_{ix}\cos\partial + p_{iy}\sin\partial\right)^2/a^2 + \left(p_{ix}\sin\partial - p_{iy}\cos\partial\right)^2/b^2 - 1$ along with p_{ix} and p_{iy}, respectively. And the $\mathbf{\Phi}_{i1}$ can be written as follows:

$$\begin{aligned}\mathbf{\Phi}_{i1} &= [\cos\beta_{i1}, \sin\beta_{i1}]^T \\ &= \left[-g_{iy}/\sqrt{g_{ix}^2 + g_{iy}^2}, g_{ix}/\sqrt{g_{ix}^2 + g_{iy}^2}\right]^T\end{aligned} \quad (6)$$

Next, to drive quadrotor team to circumnavigate with a tunable intervehicle distance, the arc distance between the i^{th} and the k^{th} quadrotors is

$$l_{ik} = \int_{\vartheta_i}^{\vartheta_k} \sqrt{\rho_{id}^2(\vartheta) + \dot{\rho}_{id}^2(\vartheta)}\, d\vartheta \quad (7)$$

where $\dot{\rho}_{id}(\vartheta)$ is formulated as

$$\dot{\rho}_{id}(\vartheta_i) = \frac{ab\left(a^2 - b^2\right)\rho_{id}(\vartheta_i)\sin(\vartheta_i - \partial)\cos(\vartheta_i - \partial)}{\left[a^2\sin^2(\vartheta_i - \partial) + b^2\cos^2(\vartheta_i - \partial)\right]^{3/2}}$$

Define relative arc lengthen error with desired arc distance l_{ik}^d as $\tilde{l}_{ik} = l_{ik} - l_{ik}^d, \forall i \neq k$ and e_{li} is

$$e_{li} = \sum_{k\in N} a_{ik}\tilde{l}_{ik} \quad (8)$$

where a directed weighted graph $G = \{V, E, A\}$ is employed to express the communication network with $V = \{1, 2, \cdots, N\}$, E denoting the edge set and $A = [a_{ik}] \in \mathbb{R}^{N\times N}$ being the adjacent matrix of G. Specifically, $a_{ij} = 1$ tells a relation that the i^{th} quadrotors can receive information from the k^{th} quadrotors, otherwise $a_{ik} = 0$. Define the radius error as $e_{i\rho} = \rho_i - \rho_{id}$ and a horizontal elliptical guidance rule is scheduled as

$$\bar{\boldsymbol{v}}_{iH} = \underbrace{k_{i1}e_{i\rho}\mathbf{\Phi}_i + \dot{\boldsymbol{p}}_t}_{\text{converging to ellipse}} + \underbrace{(\alpha + h_i)\mathbf{\Phi}_{i1}}_{\text{circling on ellipse}} \quad (9)$$

where $k_{i1} > 0$ is a user-defined constant, α is set to decide the circling direction, i.e., clockwise ($\alpha < 0$) or anticlockwise ($\alpha > 0$). h_i with a parameter $h_0 > 0$ is the term to regulate the arc lengthen between quadrotors, calculated by $h_i = h_0\tanh(e_{li})$. One can evidently find that (9) is generally separated into two portions, i.e., converging term as well as circling term, which respectively correspond to drive quadrotors to fly to the ideal relative position to target and assure the orbiting motion on the ellipse trajectory.

Remark 1: One can conclude that elliptical trajectory undoubtably owns a much broader university but sophisticated compared to suggested circular reports [18], [19], [20] not only due to the nonorthogonal feature of tangential velocity and axial velocity, but also arising from the time-varying radius concerned with $\beta_i(t)$. While it should point that elliptical circumnavigation provides unique advantage in term of improved flexibility, which are suitable for the whole circular circling scenarios and can be directly modified to standard circular orbiting by setting the equal major and minor axis values.

2) LONGITUDINAL CONTROLLER

Let the longitudinal tracking error be $e_{ipz} = p_{iz} - z_d$, where z_d corresponds to the altitude command. Differentiating e_{ipz} yields

$$\dot{e}_{ipz} = v_{iz} - \dot{z}_d \quad (10)$$

To stabilize e_{ipz}, the reference of height motion rate is derived by the height control law as

$$\bar{v}_{iz} = -k_{iz}e_{ipz} + \dot{z}_d \quad (11)$$

Furtherly, let the velocity vector of the i^{th} quadrotors as $\bar{\boldsymbol{v}}_i = \left[\bar{\boldsymbol{v}}_{iH}^T, \bar{v}_{iz}\right]^T$ and its velocity tracking is $\boldsymbol{e}_{iv} = \boldsymbol{v}_i - \bar{\boldsymbol{v}}_i = \left[e_{ivx}, e_{ivy}, e_{ivz}\right]^T$. Recalling (1), $\dot{\boldsymbol{e}}_{iv}$ is formulated as

$$\dot{\boldsymbol{e}}_{iv} = \underbrace{\left(\boldsymbol{K}_i u_{iF} - \boldsymbol{G}_i\right)/m_i}_{\boldsymbol{F}_i\left(\Theta_i^d, u_{iF}\right)} - \dot{\bar{\boldsymbol{v}}}_i \quad (12)$$

Based on (12), the velocity control input comprising of thruster and attitude reference is designed as follows:

$$\boldsymbol{F}_i^d\left(\mathbf{\Theta}_i^d, u_{iF}\right) = -k_{i2}\boldsymbol{e}_{iv} + \dot{\bar{\boldsymbol{v}}}_i \quad (13)$$

where $k_{i2} > 0$ is the control gain. $\boldsymbol{F}_i^d\left(\mathbf{\Theta}_i^d, u_{iF}\right) = \left[F_{ix}^d, F_{iy}^d, F_{iz}^d\right]^T$ represents the virtual control torque, steered by $\mathbf{\Theta}_i^d = [\phi_i^d, \theta_i^d, \psi_i^d]^T$ in orientation as well as u_{iF} in magnitude. Apply $\boldsymbol{K}_i$ on (13) yields (14), as shown at the bottom of the next page.

Invert (14) has

$$\begin{cases} u_{iF} = m_i\sqrt{\left(F_{ix}^d\right)^2 + \left(F_{iy}^d\right)^2 + \left(F_{iz}^d + g\right)^2} \\ \phi_i^d = \arcsin\left[m_i\left(F_{ix}^d\sin\left(\psi_i^d\right) - F_{iy}^d\cos\left(\psi_i^d\right)\right)/u_{iF}\right] \\ \theta_i^d = \arctan\left[\left(F_{ix}^d\cos\left(\psi_i^d\right) + F_{iy}^d\sin\left(\psi_i^d\right)\right)/\left(F_{iz}^d + g\right)\right] \end{cases} \quad (15)$$

where the reference yaw ψ_i^d is assigned by operators.

B. ROTATIONAL LEVEL

1) ATTITUDE CONTROLLER

Recalling (2), the attitude tracking error vector of the i^{th} quadrotors is $\boldsymbol{e}_{i\boldsymbol{\Theta}} = \boldsymbol{\Theta}_i - \boldsymbol{\Theta}_i^d$ and corresponding time derivative is derived as:

$$\dot{\boldsymbol{e}}_{i\boldsymbol{\Theta}} = \dot{\boldsymbol{\Theta}}_i - \dot{\boldsymbol{\Theta}}_i^d = \mathbf{x}_{i2} - \dot{\boldsymbol{\Theta}}_i^d \tag{16}$$

Given the tracking error of angular rate as

$$\boldsymbol{e}_{i\omega} = \mathbf{x}_{i2} - \bar{\boldsymbol{x}}_{i2} \tag{17}$$

where $\bar{\boldsymbol{x}}_{i2} = [\bar{x}_{i21}, \bar{x}_{i22}, \bar{x}_{i23}]^T$ denotes virtual attitude control law to be designed. (16) is updated to

$$\dot{\boldsymbol{e}}_{i\boldsymbol{\Theta}} = \boldsymbol{e}_{i\omega} + \bar{\boldsymbol{x}}_{i2} - \dot{\boldsymbol{\Theta}}_i^d \tag{18}$$

Here we design $\bar{\boldsymbol{x}}_{i2}$ as

$$\bar{\boldsymbol{x}}_{i2} = -k_{i3}\dot{\boldsymbol{e}}_{i\boldsymbol{\Theta}} + \dot{\boldsymbol{\Theta}}_i^d \tag{19}$$

Thus (18) can be updated to

$$\dot{\boldsymbol{e}}_{i\boldsymbol{\Theta}} = -k_{i3}\boldsymbol{e}_{i\boldsymbol{\Theta}} + \boldsymbol{e}_{i\omega} \tag{20}$$

Define the tracking error of angular rate as $\boldsymbol{e}_{i\omega} = \boldsymbol{x}_{i2} - \bar{\boldsymbol{x}}_{i2} = [e_{i\omega 1}, e_{i\omega 2}, e_{i\omega 3}]^T$ and its time derivative is written as

$$\dot{\boldsymbol{e}}_{i\omega} = \dot{\boldsymbol{x}}_{i2} - \dot{\bar{\boldsymbol{x}}}_{i2} = \boldsymbol{\tau}_i + \boldsymbol{\Delta}_i - \dot{\bar{\boldsymbol{x}}}_{i2} \tag{21}$$

Assumption 2: The time differential of lumped disturbance $\boldsymbol{\Delta}_i$ is bounded by an unknown but by a positive constant, mathematically described by $\sup_{t\geq 0}\|\boldsymbol{\Delta}_i\| \leq \bar{\Delta}_i$ with $\bar{\Delta}_i > 0$.

Remark 2: In practical engineering, the energy of onboard equipment as well as external perturbations are both limited, resulting in a limited motion of quadrotors. Consequently, it is reasonable to obtain that time differential of $\boldsymbol{\Delta}_i$ connected to system dynamics and extraneous uncertainties are bounded. Moreover, such upper bound $\bar{\Delta}_i$ is merely used in respect of stability analysis, rather than controller design.

2) USDE DESIGN

To guarantee robustness of the elliptical circumnavigation, an USDE is presented for quadrotors to observe the unknown $\boldsymbol{\Delta}_i$ and achieve disturbance compensation. Guided by previous works in [26], apply lower-pass filter operation $(\cdot)^f = [\cdot]/(\kappa s + 1)$ on (2), one gets

$$\begin{cases} \kappa\dot{x}_{i2jf} + x_{i2jf} = x_{i2j}, x_{i2jf}(0) = 0 \\ \kappa\dot{\tau}_{ijf} + \tau_{ijf} = \tau_{ij}, \tau_{ijf}(0) = 0 \\ \kappa\dot{\Delta}_{ijf} + \Delta_{ijf} = \Delta_{ij}, \Delta_{ijf}(0) = 0, \end{cases} \quad (j = 1, 2, 3) \tag{22}$$

where $\kappa > 0$ is a filter constant. x_{i2fj}, τ_{ifj} and Δ_{ijf} are filtered states of the quadrotor system dynamics x_{i2j}, τ_{ij} and Δ_{ij}, respectively.

Lemma 1 [24]: Construct a variable as

$$Z_{ij} = \frac{x_{i2j} - x_{i2jf}}{\kappa} - \tau_{ijf} - \Delta_{ij} \tag{23}$$

where Z_{ij} can exponentially converge to a small set and satisfying

$$\lim_{\kappa\to 0}\{\lim_{t\to+\infty}[Z_{ij}(t)]\} = 0 \tag{24}$$

which implies that $Z_{ij} = 0$ is an invariant manifold.

Therefore, following (23) and (24), the USDE for quadrotors is designed as

$$\hat{\Delta}_{ij} = \frac{x_{i2j} - x_{i2jf}}{\kappa} - \tau_{ijf} \tag{25}$$

And one has the estimation error vector $\hat{\boldsymbol{\Delta}}_i = \left[\hat{\Delta}_{i1}, \hat{\Delta}_{i2}, \hat{\Delta}_{i3}\right]^T$.

Remark 3: With a straightforward constructure, the USDE is presented for quadrotors to rebuild the lumped disturbance based on the invariant manifold, not only endowing a relaxed computing burden compared to NN-based observer but also immensely improving the system robustness against uncertainties. Additionally, from *Lemma 1*, an asymptotic convergence of USDE estimation error is assured by tuning a suitable filtering constant κ, surpassing the ESO merely offering an ultimately uniformly bounded (UUB) estimation result.

3) ANGULAR RATE CONTROLLER

Based on (21) and USDE (25), the control input to regulate angular rate of the i^{th} quadrotors is given by

$$\tau_{ij} = -k_{i4}e_{i\omega j} - \hat{\Delta}_{ij} + \dot{\bar{x}}_{i2j} \tag{26}$$

where $k_{i4} > 0$ is a nonnegative control gain.

IV. STABILITY ANALYSIS

Stability of the overall circumnavigation system containing USDE, rotational subsystem as well as translational subsystem will be analyzed in this section and input-to-state stable (ISS) results are arrived.

A. USDE

State the disturbance estimation error of USDE as $\tilde{\Delta}_{ij} = \Delta_{ij} - \hat{\Delta}_{ij}$. Differentiating $\tilde{\Delta}_{ij}$ based on (2), (22) and (25), one

$$\begin{cases} F_{ix}^d = u_{iF}\left(\cos\left(\psi_i^d\right)\sin\left(\theta_i^d\right)\cos\left(\phi_i^d\right) + \sin\left(\psi_i^d\right)\sin\left(\phi_i^d\right)\right)/m_i \\ F_{iy}^d = u_{iF}\left(\sin\left(\psi_i^d\right)\sin\left(\theta_i^d\right)\cos\left(\phi_i^d\right) - \cos\left(\psi_i^d\right)\sin\left(\phi_i^d\right)\right)/m_i \\ F_{iz}^d = u_{iF}\left(\cos\left(\theta_i^d\right)\cos\left(\phi_i^d\right)\right)/m_i - g \end{cases} \tag{14}$$

has

$$\begin{aligned}\dot{\tilde{\Delta}}_{ij} &= \dot{\Delta}_{ij} - \dot{\hat{\Delta}}_{ij} = \dot{\Delta}_{ij} - \left(\frac{\dot{x}_{i2j} - \dot{x}_{i2jf}}{\kappa} - \dot{\tau}_{ijf}\right) \\ &= \dot{\Delta}_{ij} - \frac{\dot{x}_{i2j} - \left(x_{i2j} - x_{i2jf}\right)/\kappa}{\kappa} + \dot{\tau}_{ijf} \\ &= \dot{\Delta}_{ij} - \frac{\tau_{ij} + \Delta_{ij} - \left(x_{i2j} - x_{i2jf}\right)/\kappa}{\kappa} + \frac{\tau_{ij} - \tau_{ijf}}{\kappa} \\ &= \dot{\Delta}_{ij} - \frac{\Delta_{ij}}{\kappa} + \frac{\left(x_{i2j} - x_{i2jf}\right)/\kappa - \tau_{ijf}}{\kappa} \\ &= -\frac{\tilde{\Delta}_{ij}}{\kappa} + \dot{\Delta}_{ij} \end{aligned} \tag{27}$$

Lemma 2 [19]: For USDE subsystem following Assumption 2 in (27): $\left[\Delta_{ij}\right] \mapsto \left[\tilde{\Delta}_{ij}\right]$, an ISS can be arrived.

Proof: Select a Lyapunov function as

$$V_1 = \sum_{i=1}^{N}\sum_{j=1}^{3}\left(\frac{\tilde{\Delta}_{ij}^2}{2}\right) \tag{28}$$

where the differentiation of V_1 along with time is

$$\begin{aligned}\dot{V}_1 &= \sum_{i=1}^{N}\sum_{j=1}^{3}\left[\tilde{\Delta}_{ij}\left(-\frac{\tilde{\Delta}_{ij}}{\kappa} + \dot{\Delta}_{ij}\right)\right] \\ &= \sum_{i=1}^{N}\sum_{j=1}^{3}\left(-\frac{\tilde{\Delta}_{ij}^2}{\kappa} + \tilde{\Delta}_{ij}\dot{\Delta}_{ij}\right)\end{aligned} \tag{29}$$

Recalling *Assumption* 2, (29) can be switched to

$$\dot{V}_1 \le \sum_{i=1}^{N}\sum_{j=1}^{3}\left(-\frac{\tilde{\Delta}_{ij}^2}{\kappa} + \left|\tilde{\Delta}_{ij}\right|\bar{\Delta}_i\right) \tag{30}$$

When $\left|\tilde{\Delta}_{ij}\right| \ge \kappa\bar{\Delta}_i/\chi_1, \chi_1 \in (0,1)$ is met, $\dot{V}_1$ can be rewritten as

$$\dot{V}_1 \le -\sum_{i=1}^{N}\sum_{j=1}^{3}\left[\frac{1}{\kappa}\left(1-\chi_1\right)\tilde{\Delta}_{ij}^2\right] \le -\frac{2}{\kappa}\left(1-\chi_1\right)V_1 \tag{31}$$

Thus, the error dynamics of USDE in (27) is ISS with an upper bound being

$$\left|\tilde{\Delta}_{ij}\left(t\right)\right| \le \max\left\{\varpi_1\left(\left|\tilde{\Delta}_{ij}\left(0\right)\right|, t\right), \frac{\kappa\bar{\Delta}_i}{\chi_1}\right\} \tag{32}$$

where ϖ_1 is a ***KL*** function. ■

B. ROTATIONAL SUBSYSTEM

Combining (20) and (21) yields the error dynamics of rotational subsystem, expressed as

$$\begin{cases}\dot{\boldsymbol{e}}_{i\boldsymbol{\Theta}} = -k_{i3}\boldsymbol{e}_{i\boldsymbol{\Theta}} + \boldsymbol{e}_{i\omega} \\ \dot{\boldsymbol{e}}_{i\omega} = \boldsymbol{\tau}_i + \boldsymbol{\Delta}_i - \dot{\bar{\boldsymbol{x}}}_{i2}\end{cases} \tag{33}$$

Lemma 3: Assign $\tilde{\boldsymbol{\Delta}}_i = \boldsymbol{\Delta}_i - \hat{\boldsymbol{\Delta}}_i$ as the input of (33) and one can derive that the rotational subsystem, i.e., $\left[\tilde{\boldsymbol{\Delta}}_i\right] \mapsto [\boldsymbol{e}_{i\boldsymbol{\Theta}}, \mathbf{e}_{i\omega}]$ is ISS.

Proof: Elect the Lyapunov function for rotational subsystem as and its time differential is

$$\begin{aligned}\dot{V}_2 &= \sum_{i=1}^{N}\left(e_{i\Theta}^T\dot{e}_{i\Theta} + e_{i\omega}^T\dot{e}_{i\omega}\right) \\ &= \sum_{i=1}^{N}\left[e_{i\Theta}^T\left(-k_{i3}e_{i\Theta} + e_{i\omega}\right) + e_{i\omega}^T\left(\tau_i + \Delta_i - \dot{\bar{x}}_{i2}\right)\right]\end{aligned} \tag{34}$$

Substituting (26) into (34), $\dot{V}_2$ is rewritten as

$$\dot{V}_2 = \sum_{i=1}^{N}\left[\boldsymbol{e}_{i\boldsymbol{\Theta}}^T\left(-k_{i3}\boldsymbol{e}_{i\boldsymbol{\Theta}} + \boldsymbol{e}_{i\omega}\right) + \boldsymbol{e}_{i\omega}^T\left(-k_{i4}\boldsymbol{e}_{i\omega} + \tilde{\boldsymbol{\Delta}}_i\right)\right] \tag{35}$$

Following Young's inequalities [27], one has

$$\begin{aligned}&\dot{V}_2 \\ &\le \sum_{i=1}^{N}\left\{-\left(k_{i3} - \frac{1}{2}\right)\left\|e_{i\Theta}\right\|^2 - \left(k_{i4} - 1\right)\left\|e_{i\omega}\right\|^2 + \frac{1}{2}\left\|\tilde{\Delta}_i\right\|^2\right\}\end{aligned} \tag{36}$$

Let $K_2 = \min\left\{2k_{i3} - 1, 2k_{i4} - 2\right\} > 0$ and $H_2 = \sum_{i=1}^{N}\left(\left\|\tilde{\Delta}_i\right\|^2/2\right)$ with $k_{i3} > 0.5$ and $k_{i4} > 1$ being necessary. And (37) can be simplified as

$$\dot{V}_2 \le -K_2V_2 + H_2 \tag{37}$$

Integrate (36) over $(0, t)$ gains

$$\begin{aligned}V_2(t) &\le \frac{H_2}{K_2}\left(1 - e^{-K_2t}\right) + V_2(0)e^{-K_2t} \\ &\le \sum_{i=1}^{N}\left\{\frac{\left\|\tilde{\Delta}_i\right\|^2}{2K_2}\left(1 - e^{-K_2t}\right) + \frac{\left\|\boldsymbol{E}_{i\Theta}(0)\right\|^2}{2}e^{-K_2t}\right\}\end{aligned} \tag{38}$$

where $\boldsymbol{E}_{i\boldsymbol{\Theta}} = \left[\boldsymbol{e}_{i\boldsymbol{\Theta}}^T, \boldsymbol{e}_{i\omega}^T\right]^T$. Next, it can be evidently attained that

$$\left\|\boldsymbol{E}_{i\boldsymbol{\Theta}}\left(t\right)\right\| \le \sqrt{\frac{\left\|\tilde{\boldsymbol{\Delta}}_i\right\|^2\left(1 - e^{-K_2t}\right)}{K_2}} + \left\|\boldsymbol{E}_{i\boldsymbol{\Theta}}\left(0\right)\right\|\sqrt{e^{-K_2t}} \tag{39}$$

Under *Lemma 2*, the boundary of $\left\|\boldsymbol{E}_{i\boldsymbol{\Theta}}\left(t\right)\right\|$ is

$$\left\|\boldsymbol{E}_{i\boldsymbol{\Theta}}\left(t\right)\right\| \le \max\left\{\left\|\boldsymbol{E}_{i\boldsymbol{\Theta}}\left(0\right)\right\|\sqrt{e^{-K_2t}}, \left\|\tilde{\boldsymbol{\Delta}}_i\right\|\Big/\sqrt{K_2}\right\} \tag{40}$$

Thus, the rotational subsystem (33) is ISS. ■

C. TRANSLATIONAL SUBSYSTEM

For translational subsystem, the time differential of $e_{i\rho}$ can be deduced as

$$\begin{aligned}\dot{e}_{i\rho} &= \dot{\rho}_i - \dot{\rho}_{id} = \frac{1}{\rho_i}\left(\dot{\boldsymbol{p}}_{iH}^T - \dot{\boldsymbol{p}}_t^T\right)\left(\boldsymbol{p}_{iH} - \boldsymbol{p}_t\right) - \dot{\rho}_{id} \\ &= -\left[\boldsymbol{e}_{ivH}^T + k_{i1}e_{i\rho}\boldsymbol{\Phi}_i + \left(\alpha + h_i\right)\boldsymbol{\Phi}_{i1}\right]\boldsymbol{\Phi}_i - \dot{\rho}_{id} \\ &= -k_{i1}e_{i\rho} - \boldsymbol{e}_{ivH}^T\boldsymbol{\Phi}_i - \left(\alpha + h_i\right)\boldsymbol{\Phi}_{i1}^T\boldsymbol{\Phi}_i - \dot{\rho}_{id}\end{aligned} \tag{41}$$

where $\boldsymbol{e}_{ivH} = \left[e_{ivx}, e_{ivy}\right]^T$. State the coupling error as $\tilde{\boldsymbol{F}}_i = \left(\boldsymbol{K}_i u_{iF} - \boldsymbol{G}_i\right)/m_i - \boldsymbol{F}_i^d$, which is Lipschitz and continuous, obeying $\left\|\tilde{\boldsymbol{F}}_i\right\| \leq K_{iF} \left\|\boldsymbol{e}_{i\boldsymbol{\Theta}}\right\|$ with K_{iF} being a positive scalar. Then utilize (41) and substituting (11), (13) into (10), (12) yields the error dynamics of the translational subsystem as:

$$\begin{cases} \dot{e}_{i\rho} = -k_{i1} e_{i\rho} - \boldsymbol{e}_{ivH}^T \boldsymbol{\Phi}_i - (\alpha + h_i)\, \boldsymbol{\Phi}_{i1}^T \boldsymbol{\Phi}_i - \dot{\rho}_{id} \\ \dot{e}_{ipz} = -k_{ipz} e_{ipz} - e_{ivz} \\ \dot{\boldsymbol{e}}_{iv} = -k_{i2} \boldsymbol{e}_{iv} + \tilde{\boldsymbol{F}}_i \end{cases} \tag{42}$$

Lemma 4: Based on *Assumption 1* and *Lemma 3*, the translational subsystem (42): $\left[\boldsymbol{e}_{i\boldsymbol{\Theta}}\right] \mapsto \left[e_{i\rho}, e_{ipz}, \boldsymbol{e}_{iv}\right]$ is ISS. Meanwhile, the control objective a), i.e., $\lim_{t\to\infty} \left|e_{i\rho}(t)\right| \leq \varepsilon_1, \forall i = 1, 2, \cdots, N$ as well as $im_{t\to\infty} |e_{il}(t)| \leq \varepsilon_2, \forall i = 1, 2, \cdots, N$, can be realized.

Proof: Design the Lyapunov function of translational subsystem as $V_3 = \sum_{i=1}^N \left[\left(e_{i\rho}^2 + e_{ipz}^2 + \boldsymbol{e}_{iv}^T \boldsymbol{e}_{iv}^2\right)/2\right]$. Take the differentiation of V_3 with time has

$$\begin{aligned} &\dot{V}_3 \\ &= \sum_{i=1}^N \left(e_{i\rho}\dot{e}_{i\rho} + e_{ipz}\dot{e}_{ipz} + \boldsymbol{e}_{iv}^T \dot{\boldsymbol{e}}_{iv}\right) \\ &= \sum_{i=1}^N \left\{ \begin{array}{l} e_{i\rho}\left[-k_{i1} e_{i\rho} - \boldsymbol{e}_{ivH}^T \boldsymbol{\Phi}_i \right. \\ \left. -(\alpha + h_i)\, \boldsymbol{\Phi}_{i1}^T \boldsymbol{\Phi}_i - \dot{\rho}_{id}\right] \\ +e_{ipz}\left(-k_{ipz} e_{ipz} - e_{ivz}\right) + \boldsymbol{e}_{iv}^T \left(-k_{i2}\boldsymbol{e}_{iv} + \tilde{\boldsymbol{F}}_i\right) \end{array} \right\} \\ &= \sum_{i=1}^N \left\{ \begin{array}{l} -k_{i1} e_{i\rho}^2 - k_{ipz} e_{ipz}^2 - k_{i2} \boldsymbol{e}_{iv}^T \boldsymbol{e}_{iv} \\ -e_{i\rho}\left[\boldsymbol{e}_{ivH}^T \boldsymbol{\Phi}_i + (\alpha + h_i)\, \boldsymbol{\Phi}_{i1}^T \boldsymbol{\Phi}_i + \dot{\rho}_{id}\right] \\ -e_{ipz} e_{ivz} + \boldsymbol{e}_{iv}^T \tilde{\boldsymbol{F}} \end{array} \right\} \end{aligned} \tag{43}$$

Note that $h_i = h_0 \tanh(e_{li})$ is naturally bounded. Meanwhile, under *Assumption 1*, the boundness of $\dot{\rho}_{id}$ can also be attained. Hence, one has $|h_i| \leq \bar{h}_1$ and $|\dot{\rho}_{id}| \leq \bar{h}_2$ with $\bar{h}_1$ and $\bar{h}_2$ being positive scalars. Combining $\left\|\tilde{\boldsymbol{F}}_i\right\| \leq K_{iF} \left\|\boldsymbol{e}_{i\boldsymbol{\Theta}}\right\|$ and the property of Young's inequalities, (44) can be further deduced as

$$\begin{aligned} \dot{V}_3 &\leq \sum_{i=1}^N \left\{ \begin{array}{l} -k_{i1} e_{i\rho}^2 - k_{ipz} e_{ipz}^2 - k_{i2} e_{iv}^T e_{iv} \\ +\left|e_{i\rho}\right| \left(\left\|e_{ivH}\right\| + |\alpha| + \bar{h}_1 + \bar{h}_2\right) \\ -e_{ipz} e_{inz} + K_{iF} \left\|e_{i\Theta}\right\| \left\|e_{iv}\right\| \end{array} \right\} \\ &\leq \sum_{i=1}^N \left\{ \begin{array}{l} -\left(k_{i1} - 0.5\right) e_{i\rho}^2 - \left(k_{ipz} - 0.5\right) e_{ipz}^2 \\ \quad -\left(k_{i2} - 1\right) e_{iv}^T e_{iv} \\ +\left|e_{i\rho}\right| \left(|\alpha| + \bar{h}_1 + \bar{h}_2\right) + K_{iF} \left\|e_{i\Theta}\right\| \left\|e_{iv}\right\| \end{array} \right\} \end{aligned} \tag{44}$$

Let $K_{i3} = \min\left\{k_{i1} - 0.5, k_{ipz} - 0.5, k_{i2} - 1\right\} > 0$ and $\boldsymbol{e}_{i3} = \left[e_{i\rho}, e_{ipz}, \boldsymbol{e}_{iv}^T\right]^T$, then invoking K_{i3} and $\boldsymbol{E}_{i3}$ into (44) gets

$$\dot{V}_3 \leq \sum_{i=1}^N \left[K_{i3} \left\|E_{i3}\right\|^2 + \left\|E_{i3}\right\| \left(|\alpha| + \bar{h}_1 + \bar{h}_2 + K_{iF} \left\|e_{i\Theta}\right\|\right)\right] \tag{45}$$

when $\left\|\boldsymbol{E}_{i3}\right\| \geq \left(|\alpha| + \bar{h}_1 + \bar{h}_2 + K_{iF} \left\|\boldsymbol{e}_{i\boldsymbol{\Theta}}\right\|\right)/(K_{i3}\mathcal{X}_2)$, $\mathcal{X}_2 \in (0, 1)$ is fulfilled, one has

$$\dot{V}_3 \leq \sum_{i=1}^N \left[-K_{i3}\left(1 - \chi_2\right) \left\|\boldsymbol{E}_{i3}\right\|^2\right] \tag{46}$$

Evidently, under *Lemma 3*, the upper boundary of $\left\|\boldsymbol{E}_{i3}\right\|$ is attained as

$$\begin{aligned} &\left\|\boldsymbol{E}_{i3}(t)\right\| \\ &\leq \max\left\{\varpi_2\left(\left\|\boldsymbol{E}_{i3}(0)\right\|, t\right), \frac{|\alpha| + \bar{h}_1 + \bar{h}_2 + K_{iF}\left\|\boldsymbol{e}_{i\boldsymbol{\Theta}}\right\|}{K_{i3}\chi_2}\right\} \end{aligned} \tag{47}$$

where ϖ_2 is a $\boldsymbol{KL}$ function. Therefore, one can derive that the quadrotors are assured to enclose the target with a desired relative distance, i.e., $\lim_{t\to\infty} \left|e_{i\rho}(t)\right| \leq \varepsilon_1, \forall i = 1, 2, \cdots, N$ is accomplished.

Subsequent analysis is presented to ensure $\text{im}_{t\to\infty} |e_{il}(t)| \leq \varepsilon_2, \forall i = 1, 2, \cdots, N$. Define a matrix as $\boldsymbol{C} = [0, -1; 1, 0]$ and one has

$$\vartheta_i = \beta_i = \arctan\left(\frac{p_{iy} - p_{ty}}{p_{ix} - p_{tx}}\right) \tag{48}$$

And the derivative of ϑ_i can be attained as

$$\begin{aligned} \dot{\vartheta}_i &= \frac{\left(\dot{p}_{iy} - \dot{p}_{ty}\right)\left(p_{ix} - p_{tx}\right) - \left(p_{iy} - p_{ty}\right)\left(\dot{p}_{ix} - \dot{p}_{tx}\right)}{\left(p_{ix} - p_{tx}\right)^2 + \left(p_{iy} - p_{ty}\right)^2} \\ &= \frac{\left(\dot{\boldsymbol{p}}_t^T - \dot{\boldsymbol{p}}_{iH}^T\right) \boldsymbol{C} \left(\boldsymbol{p}_t - \boldsymbol{p}_{iH}\right)}{\rho_i^2} = \frac{\left(\dot{\boldsymbol{p}}_t^T - \boldsymbol{v}_{iH}^T\right) \boldsymbol{C} \boldsymbol{\Phi}_i}{\rho_i} \\ &= -\boldsymbol{e}_{ivH}^T \boldsymbol{C} \boldsymbol{\Phi}_i + \frac{(\alpha + h_i)}{\rho_i} \sin\left(\beta_i - \beta_{i1}\right) \end{aligned} \tag{49}$$

Note that $\boldsymbol{e}_{ivH}$ is bounded and can converge to a tiny set by set a big control gain, which has been proved in previous analysis. Hence one has

$$\dot{\vartheta}_i = \frac{(\alpha + h_i)}{\rho_i} \sin\left(\beta_i - \beta_{i1}\right) \tag{50}$$

Recalling the definition of e_{li} in (7) and (8), the time derivative of e_{li} can be computed as

$$\begin{aligned} &\dot{e}_{li} \\ &= \sum_{k=1}^N a_{ik} \left[\begin{array}{l} \sqrt{\rho_{kd}^2(\vartheta_k) + \dot{\rho}_{kd}^2(\vartheta_k)}\, \frac{\alpha + h_k(e_{lk})}{\rho_k} \sin\left(\beta_k - \beta_{k1}\right) \\ -\sqrt{\rho_{id}^2(\vartheta_k) + \dot{\rho}_{id}^2(\vartheta_k)}\, \frac{\alpha + h_i(e_{li})}{\rho_i} \sin\left(\beta_i - \beta_{i1}\right) \end{array} \right] \end{aligned} \tag{51}$$

Define a series of vectors as shown in the equation at the bottom of the next page, and the cooperative error dynamic can be rewritten as

$$\dot{\mathbf{E}}_l = -L\mathbf{X}_\vartheta \mathbf{H}\left(\mathbf{E}_l\right) - L\mathbf{X}_\vartheta \mathbf{P} \tag{52}$$

where $L = D - A$ with $D = diag\left(d_1, \cdots, d_n\right)$ and $d_i = \sum_{k=1}^N a_{ik}$. To analysis e_{li}, the sign of $\sin\left(\beta_i - \beta_{i1}\right)$ is essential. Substituting (3) into (5) has

$$\rho_{id}\left(\beta_i\right) = \frac{ab}{\sqrt{a^2 \sin^2\left(\beta_i - \partial\right) + b^2 \cos^2\left(\beta_i - \partial\right)}} \tag{53}$$

According to (50), $\tanh\left(\beta_{i1}\right)$ satisfies

$$\begin{aligned} \left|\tanh\left(\beta_{i1}\right)\right| &= \left|\frac{d\rho_{id}(\vartheta_i)\sin\vartheta_i}{d\vartheta_i} \frac{d\vartheta_i}{d\rho_{id}(\vartheta_i)\cos\vartheta_i}\right| \\ &= \left|\frac{a^2 \sin\left(\beta_i - \partial\right)\sin\partial - b^2\cos\left(\beta_i - \partial\right)\cos\partial}{a^2 \sin\left(\beta_i - \partial\right)\cos\partial + b^2\cos\left(\beta_i - \partial\right)\sin\partial}\right| \end{aligned} \tag{54}$$

where corresponding $\sin(\beta_i - \beta_{i1})$ can be deduced as

$$\begin{cases} \sin\beta_{i1} = \dfrac{a^2\sin(\beta_i-\partial)\sin\partial - b^2\cos(\beta_i-\partial)\cos\partial}{\sqrt{a^4\sin^2(\beta_i-\partial)+b^4\cos^2(\beta_i-\partial)}} \\ \cos\beta_{i1} = \dfrac{a^2\sin(\beta_i-\partial)\cos\partial + b^2\cos(\beta_i-\partial)\sin\partial}{\sqrt{a^4\sin^2(\beta_i-\partial)+b^4\cos^2(\beta_i-\partial)}} \end{cases} \tag{55}$$

Then the $\sin(\beta_i - \beta_{i1})$ can be attained as

$$\sin(\beta_i-\beta_{i1}) = \frac{a^2\sin^2(\beta_i-\partial)+b^2\cos^2(\beta_i-\partial)}{\sqrt{a^4\sin^2(\beta_i-\partial)+b^4\cos^2(\beta_i-\partial)}} \tag{56}$$

Evidently, it can be found that $\sin(\beta_i-\beta_{1i})\sqrt{\rho_{id}^2(\vartheta_i)+\dot\rho_{id}^2(\vartheta_i)}\Big/\rho_i > 0$. And under *Lemmas 1-3* and previous discussion, the cooperative arc lengthen error e_{li} can arrived at a UUB stability and $\mathrm{im}_{t\to\infty}|e_{il}(t)| \le \varepsilon_2, \forall i = 1, 2, \cdots, N$ is validated. ■

Theorem 1: For the overall elliptical circumnavigation control strategy for quadrotors (1) containing guidance rule (9), longitudinal control law (11), 3-D velocity control input (13), attitude control rule (19), angular rate control torque (26) and USDE (25), all the error dynamics are bounded under *Assumptions 1-2*.

Proof: See *Lemmas 2-4*. ■

Remark 4: With the aim of convenient controller implementation, the parameter tuning guideline is outlined as:

1) For translational subsystem, larger k_{i1}, k_{ipz} and k_{i2} play important roles in constraining $\|\boldsymbol{E}_{i3}\|$, resulting in a fast as well as accurate enclosing and elliptical circumnavigation for quadrotors. However, extremely large control gains may induce transient fluctuations. Consequently, it is suggested to properly selecting those gains. Moreover, for h_i, a compromise between relative arc lengthen error and enclosing error should be made carefully.

2) For rotational subsystem, the amplitude of $\|\boldsymbol{E}_{i\boldsymbol{\Theta}}\|$ is related to k_{i3} and k_{i4}. Bigger k_{i3} and k_{i4} contribute an accelerated attitude tracking error convergence and a small $\|\boldsymbol{E}_{i\boldsymbol{\Theta}}\|$. But similarly, excessively huge k_{i3}, k_{i4} will result in chattering at transient phase. Thus, one should modulate suitable k_{i3} and k_{i4} in scale.

3) For USDE, although a minor filter constant κ is recommended in obtaining a precise disturbance observation, the increased sensitivity to sensor noise may arise unexpected oscillations, thus a proper value should be adjusted to obtain an improved robustness for quadrotor team.

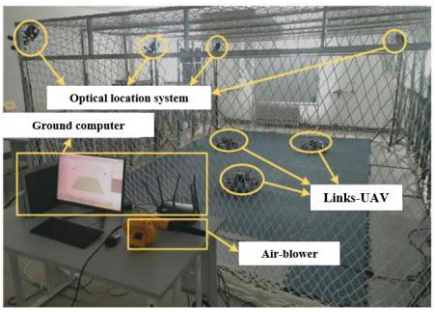

FIGURE 4. The experimental test rig.

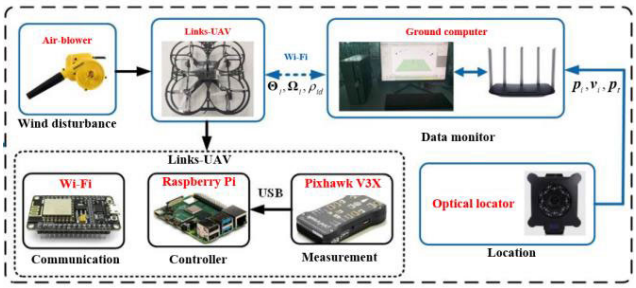

FIGURE 5. Relation of system modules.

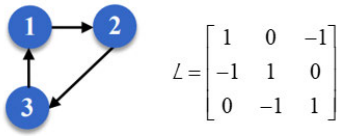

$$\mathcal{L} = \begin{bmatrix} 1 & 0 & -1 \\ -1 & 1 & 0 \\ 0 & -1 & 1 \end{bmatrix}$$

FIGURE 6. Directed communication topology for quadrotor team.

V. EXPERIMENT RESULTS

A. EXPERIMENT ENVIRONMENT

To verify the effectiveness and feasibility of proposed elliptical circumnavigation control algorithm, some experiments are carried out based on the Links-UAV Indoor system produced by Beijing Links Co., Ltd., and corresponding experimental rig and relation of modules are illustrated in Figs. 4-5. The system is mainly compromised by three Links UAVs, an optical location subsystem and a ground monitoring computer. Wind disturbance are generated by an air-blower. Each

$$\begin{cases} \boldsymbol{E}_l = [e_{l1}, e_{l2}, \cdots, e_{ln}]^T, \\ \mathbf{H}(\mathbf{E}_l) = [h_1(e_{l1}), h_2(e_{l2}), \cdots, h_n(e_{ln})]^T, \\ \mathbf{X}_\vartheta = diag\left(\begin{matrix} \sin(\beta_1-\beta_{11})\sqrt{\rho_{1d}^2(\vartheta_1)+\dot\rho_{1d}^2(\vartheta_1)}\Big/\rho_1, \cdots, \\ \sin(\beta_n-\beta_{1n})\sqrt{\rho_{nd}^2(\vartheta_n)+\dot\rho_{nd}^2(\vartheta_n)}\Big/\rho_n \end{matrix}\right), \\ \mathbf{P} = [\alpha, \alpha, \cdots, \alpha]^T \in \mathbb{R}^{N\times 1} \end{cases}$$

TABLE 1. Parameters of presented control algorithm.

Section	Values
Translational controller	$k_{11}=k_{21}=k_{31}=12$ $k_{1pz}=k_{2pz}=k_{3pz}=10$ $k_{12}=1.3, k_{22}=1.81, k_{32}=1.7$
Rotational controller	$\kappa=1.51$
USDE	$k_{13}=k_{23}=k_{33}=12$ $k_{14}=1.12, k_{24}=1.09, k_{34}=1.13$

FIGURE 7. Experiment process.

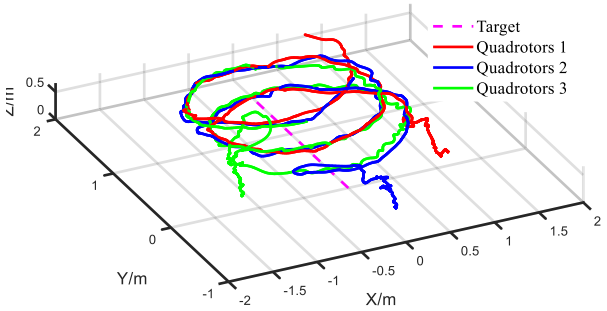

FIGURE 8. 3-D elliptical circumnavigation performances.

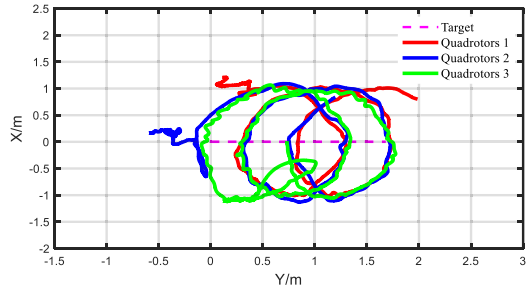

FIGURE 9. 2-D elliptical circumnavigation performances.

Links-UAV is equipped with a Pixhawk V3X, two inertial measurement units (IMUs), an onboard Raspberry Pi and a Wi-Fi module connected to the computer at a communication frequency of 2.4Ghz. The optical location subsystem is able to locate the positions of all quadrotors with a centimeter-level accuracy. Quadrotor attitudes as well as angular rates are measured by the embedded IMUs and sampled by Pixhawk V3X every 4ms.

B. EXPERIMENTAL VALIDATION

In this subsection, three Link-UAVs are utilized and the communication topology of the quadrotor tram is drawn as Fig.6. Physical characteristics of quadrotors are listed as: weight $m_i = 1.8kg$, $(i = 1, 2, 3)$, local gravitational acceleration $g = 9.8m/s^2$, distance from propeller to the quadrotor mass center $l_i = 26cm$, inertia moments $\boldsymbol{I}_i = \text{diag}(0.23, 0.21, 0.39)kg \cdot m^2$. The air-blower generates wind of $3m/s$, which

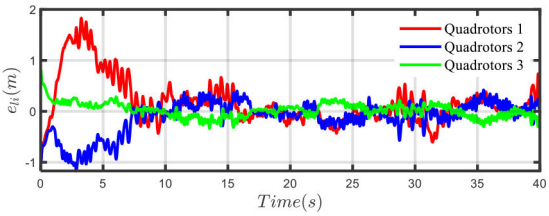

FIGURE 10. The arc distance error among quadrotors.

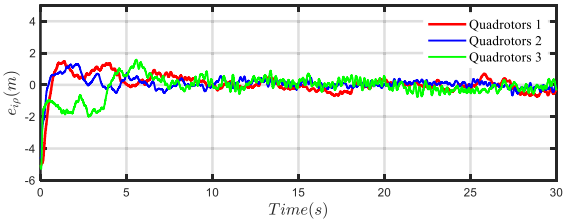

FIGURE 11. The arc distance error among quadrotors.

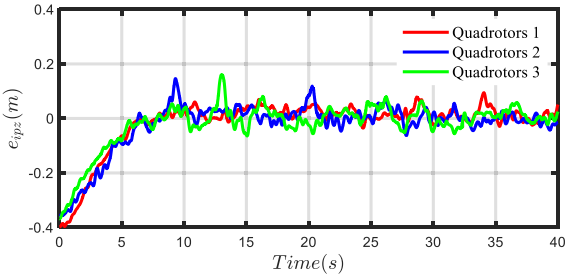

FIGURE 12. The height tracking error for quadrotors.

is deemed as the extraneous disturbances. Initial positions of three quadrotors are random on the ground with $\boldsymbol{v}_i = [0, 0, 0]^T\ m/s$. Set the virtual target move along $p_{tx} = 0, p_{ty} = 0.04t$ with a start position $(0, 0)$. The desired height is $z_d = 0.5m$ and reference of ψ_i is $\psi_i^d = 0\text{rad}$. Parameters about elliptic orbiting trajectory are $a = 0.8, b = 1, \partial = 90°, \alpha = -2, h_0 = 3$ and the ideal arc distance among quadrotors are set as $0.8m$.

Under the control parameters collected in Tab.1, experiment results are displayed in Figs. 7-12. From Figs. 7-9 showing different views of the orbiting motion, one can see that proposed encircling controller assures a great elliptical circling performance for the quadrotor team towards a moving target against wind disturbances. In Fig. 10, the inter-vehicle arc distance errors are also stabilized and quadrotors are separated spatially, such that collide could be averted. In addition, from Figs. 11-12 one can find that not only a precise translational tracking is achieved, but also offers a fast transient convergence by assigning suitable parameters under the guideline of *Remark 4*.

VI. CONCLUSION

In this paper, an USDE-based elliptical circumnavigation control scheme with a regulatable relative distance between quadrotors is proposed for quadrotor formation. With the aid of USDE, both the internal as well as external uncertainties

are observed and compensated, such that an improved robustness is endowed to quadrotor formulation. By using the arc distance, a novel elliptical orbiting guidance law is suggested, assuring a safe tracking and circling towards target.

In future, our work will focus on the elliptical circling control for quadrotor formulation with multiple targets rather than one. Another focus is that to extend proposed control scheme to handle circling scenario with unknown targets.

REFERENCES

[1] B. H. Sababha, A. Al-Mousa, R. Baniyounisse, and J. Bdour, "Sampling-based unmanned aerial vehicle air traffic integration, path planning, and collision avoidance," *Int. J. Adv. Robot. Syst.*, vol. 19, no. 2, Mar. 2022.

[2] R. M. Rolly, P. Malarvezhi, and T. D. Lagkas, "Unmanned aerial vehicles: Applications, techniques, and challenges as aerial base stations," *Int. J. Distrib. Sensor Netw.*, vol. 18, no. 9, Sep. 2022.

[3] K. Park and R. Ewing, "The usability of unmanned aerial vehicles (UAVs) for pedestrian observation," *J. Planning Educ. Res.*, vol. 42, no. 2, pp. 206–217, Jun. 2022.

[4] W. Lu, Y. Ding, Y. Gao, S. Hu, Y. Wu, N. Zhao, and Y. Gong, "Resource and trajectory optimization for secure communications in dual unmanned aerial vehicle mobile edge computing systems," *IEEE Trans. Ind. Informat.*, vol. 18, no. 4, pp. 2704–2713, Apr. 2022.

[5] Z. Zuo, C. Liu, Q.-L. Han, and J. Song, "Unmanned aerial vehicles: Control methods and future challenges," *IEEE/CAA J. Autom. Sinica*, vol. 9, no. 4, pp. 601–614, Apr. 2022.

[6] A. Akhtar, S. Saleem, and J. Shan, "Path following of a quadrotor with a cable-suspended payload," *IEEE Trans. Ind. Electron.*, vol. 70, no. 2, pp. 1646–1654, Feb. 2023.

[7] T. Huang, T. Li, and C. L. P. Chen, "Adaptive tracking control for a quadrotor system subject to internal and external uncertainties," *IEEE Trans. Circuits Syst. II, Exp. Briefs*, vol. 70, no. 3, pp. 1099–1103, Mar. 2023.

[8] T. Huang and T. Li, "Attitude tracking control of a quadrotor UAV subject to external disturbance with L_2 performance," *Nonlinear Dyn.*, vol. 111, no. 11, pp. 10183–10200, Jun. 2023.

[9] J. Jia, X. Chen, W. Wang, and M. Zhang, "Distributed control of target cooperative encirclement and tracking using range-based measurements," *Asian J. Control*, May 2023, doi: 10.1002/asjc.3124.

[10] H. Chen, K. Chang, and C. S. Agate, "UAV path planning with Tangent-plus-Lyapunov vector field guidance and obstacle avoidance," *IEEE Trans. Aerosp. Electron. Syst.*, vol. 49, no. 2, pp. 840–856, Apr. 2013.

[11] A. A. Pothen and A. Ratnoo, "Curvature-constrained Lyapunov vector field for standoff target tracking," *J. Guid., Control, Dyn.*, vol. 40, no. 10, pp. 2729–2736, Oct. 2017.

[12] E. W. Frew, D. A. Lawrence, and S. Morris, "Coordinated standoff tracking of moving targets using Lyapunov guidance vector fields," *J. Guid., Control, Dyn.*, vol. 31, no. 2, pp. 290–306, Mar. 2008.

[13] T.-H. Kim and T. Sugie, "Cooperative control for target-capturing task based on a cyclic pursuit strategy," *Automatica*, vol. 43, no. 8, pp. 1426–1431, Aug. 2007.

[14] Y. Cao, J. Muse, D. Casbeer, and D. Kingston, "Circumnavigation of an unknown target using UAVs with range and range rate measurements," in *Proc. 52nd IEEE Conf. Decis. Control*, Dec. 2013, pp. 3617–3622.

[15] C. Zhang, Y. Li, G. Qi, and A. Sheng, "Distributed finite-time control for coordinated circumnavigation with multiple non-holonomic robots," *Nonlinear Dyn.*, vol. 98, no. 1, pp. 573–588, Oct. 2019.

[16] F. Dong, K. You, and J. Zhang, "Flight control for UAV loitering over a ground target with unknown maneuver," *IEEE Trans. Control Syst. Technol.*, vol. 28, no. 6, pp. 2461–2473, Nov. 2020.

[17] F. Che, Y. Niu, J. Li, and L. Wu, "Cooperative standoff tracking of moving targets using modified Lyapunov vector field guidance," *Appl. Sci.*, vol. 10, no. 11, p. 3709, May 2020.

[18] X. Shao, J. Liu, and D. Li, "Cooperative formation control method of multiple quadrotors for stand-off tracking ground target," *Unmanned Syst. Technol.*, vol. 3, no. 1, pp. 11–18, Jan. 2020.

[19] X. Yue, X. Shao, and W. Zhang, "Elliptical encircling of quadrotors for a dynamic target subject to aperiodic signals updating," *IEEE Trans. Intell. Transp. Syst.*, vol. 23, no. 9, pp. 14375–14388, Sep. 2022.

[20] X. Peng, K. Guo, X. Li, and Z. Geng, "Cooperative moving-target enclosing control for multiple nonholonomic vehicles using feedback linearization approach," *IEEE Trans. Syst., Man, Cybern. Syst.*, vol. 51, no. 8, pp. 4929–4935, Aug. 2021.

[21] C. Song, C. Wei, F. Yang, and N. Cui, "High-order sliding mode-based fixed-time active disturbance rejection control for quadrotor attitude system," *Electronics*, vol. 7, no. 12, p. 357, Nov. 2018.

[22] R. García-Rodríguez and V. Parra-Vega, "A neuro-sliding mode control scheme for constrained robots with uncertain Jacobian," *J. Intell. Robotic Syst.*, vol. 54, no. 5, pp. 689–708, May 2009.

[23] H. Ríos, R. Falcón, O. A. González, and A. Dzul, "Continuous sliding-mode control strategies for quadrotor robust tracking: Real-time application," *IEEE Trans. Ind. Electron.*, vol. 66, no. 2, pp. 1264–1272, Feb. 2019.

[24] J. Na, B. Jing, Y. Huang, G. Gao, and C. Zhang, "Unknown system dynamics estimator for motion control of nonlinear robotic systems," *IEEE Trans. Ind. Electron.*, vol. 67, no. 5, pp. 3850–3859, May 2020.

[25] S. Wang, L. Tao, Q. Chen, J. Na, and X. Ren, "USDE-based sliding mode control for servo mechanisms with unknown system dynamics," *IEEE/ASME Trans. Mechatronics*, vol. 25, no. 2, pp. 1056–1066, Apr. 2020.

[26] L. Xu, X. Shao, and W. Zhang, "USDE-based continuous sliding mode control for quadrotor attitude regulation: Method and application," *IEEE Access*, vol. 9, pp. 64153–64164, 2021.

[27] H. Chen, X. Shao, L. Xu, and R. Jia, "Finite-time attitude control with chattering suppression for quadrotors based on high-order extended state observer," *IEEE Access*, vol. 9, pp. 159724–159733, 2021.

HAO CHEN was born in Shanxi, China, in 1995. He received the B.Sc. degree in instrument science and technology from the China University of Mining and Technology (Beijing). He is currently pursuing the Doctor of Philosophy degree in mechanical engineering, with a focus on encircling control of unmanned aerial vehicle systems, which is his primary research interest.

XINGLING SHAO (Member, IEEE) received the M.S. degree in instrument science and technology from the North University of China, Shanxi, China, in 2012, and the Doctor of Philosophy degree in navigation, guidance, and control from Beihang University, Beijing, China, in 2016. He is currently a Professor with the Department of Instrument and Electronics, North University of China, where he has been teaching, since 2018. His research interests include anti-disturbance control theory and its application on nonlinear uncertain systems, advanced signal processing methods for navigation, and robust cooperative flight control theory and method for quadrotors. He has published numerous research papers and articles on these topics in various academic journals and conferences.

RUIQING JIA was born in Shanxi, China, in 1958. He is currently a Professor with the China University of Mining and Technology (Beijing), where he holds a position with the School of Mechanical Electronic and Information Engineering. His research interest includes robotic control.